

FreshMem: Brain-Inspired Frequency-Space Hybrid Memory for Streaming Video Understanding

Kangcong Li¹ Peng Ye^{2,3} Lin Zhang¹ Chao Wang¹ Huafeng Qin⁴ Tao Chen^{*1,5}

Abstract

Transitioning Multimodal Large Language Models (MLLMs) from offline to online streaming video understanding is essential for continuous perception. However, existing methods lack flexible adaptivity, leading to irreversible detail loss and context fragmentation. To resolve this, we propose **FreshMem**, a Frequency-Space Hybrid Memory network inspired by the brain’s logarithmic perception and memory consolidation. FreshMem reconciles short-term fidelity with long-term coherence through two synergistic modules: Multi-scale Frequency Memory (MFM), which projects overflowing frames into representative frequency coefficients, complementing by residual details to reconstruct a global historical “gist”; and Space Thumbnail Memory (STM), which discretizes the continuous stream into episodic clusters by employing an adaptive compression strategy to distill them into high-density space thumbnails. Extensive experiments show that FreshMem significantly boosts the Qwen2-VL baseline, yielding gains of 5.20%, 4.52%, and 2.34% on StreamingBench, OV-Bench, and OVO-Bench, respectively. As a training-free solution, FreshMem outperforms several fully fine-tuned methods, offering a highly efficient paradigm for long-horizon streaming video understanding.

1. Introduction

Multimodal Large Language Models (MLLMs) (Yang et al., 2023; Achiam et al., 2023; Wang et al., 2024; Chen et al., 2024b) have witnessed remarkable progress in long video

understanding (Li et al., 2024c; Zhang et al., 2024b; Shen et al., 2024), demonstrating sophisticated comprehension and reasoning capabilities across diverse tasks. However, most existing methods predominantly operate under an offline paradigm (Song et al., 2024; He et al., 2024), analyzing video sequences as static, complete entities with a priori access to the entire temporal context. As MLLMs gravitate toward more dynamic and interactive environments, there is an urgent need to transition from such post-hoc analysis to online streaming video understanding (Chen et al., 2024a; Huang et al., 2025). This shift represents a fundamental evolution toward continuous perception, requiring models to reason over information as it unfolds under strict causal constraints. Thus, a key challenge emerges in maintaining a delicate balance between long-term information preservation and the seamless integration of novel, incoming frames, which is vital for MLLMs to achieve robust streaming video understanding.

Existing works have primarily evolved along two trajectories: input-level modulation (Xu et al., 2025b; Chatterjee et al., 2025), which manages data influx by merging or sparsifying frames, and memory-augmented architectures, which utilize mechanisms like KV cache eviction (Di et al., 2025; Ning et al., 2025), global memory tokens condensation (Qian et al., 2024; Zeng et al., 2025), or external memory bank construction (Xiong et al., 2025; Zhang et al., 2024a). While these methods mitigate computational pressure, they often precipitate an irrevocable loss of fine-grained details or struggle to reconcile short-term temporal fidelity with long-term contextual coherence. A fundamental limitation remains in their uniform treatment of temporal dynamics, which relies on rigid heuristics or static downsampling. Consequently, current frameworks lack the flexibility to adaptively adjust representation density over time. As the temporal horizon extends, insufficient memory consolidation leads to fragmented representations, compromising action continuity and semantic consistency, and ultimately limiting the model’s ability to sustain a coherent long-horizon narrative.

To address these structural deficiencies, we draw inspiration from the brain’s memory mechanisms, which effectively reconcile above bottleneck via two core mechanisms: loga-

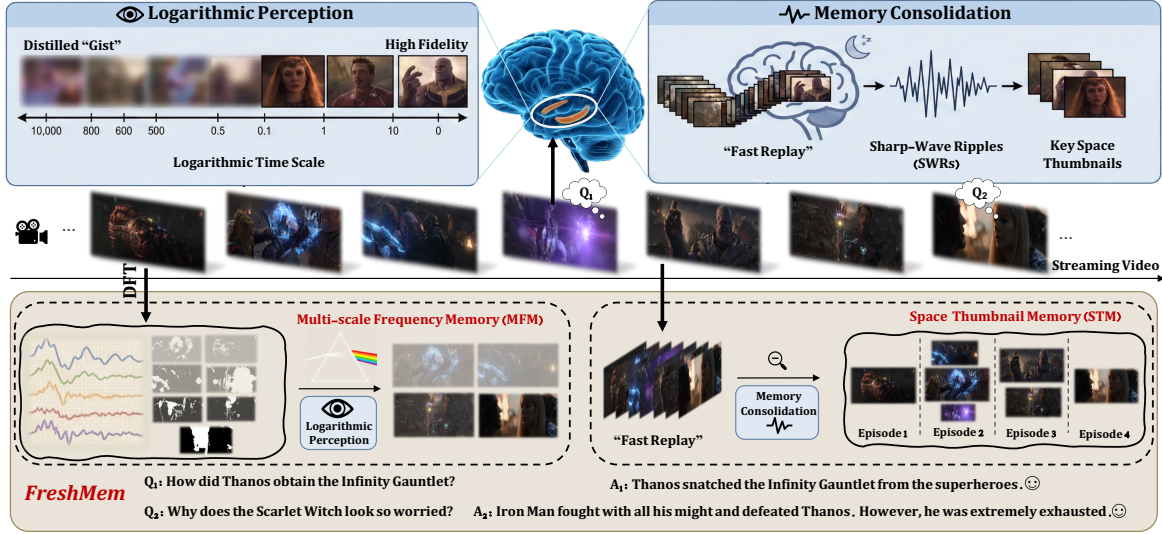


Figure 1. Overview of FreshMem and its biological foundations. (Top-Left) Logarithmic Perception, where the brain maintains high fidelity for immediate stimuli while distilling the distant past into a semantic “gist”; (Top-Right) Memory Consolidation, where SWRs compress continuous experiences into key space thumbnails; (Bottom) FreshMem materializes these principles via two synergistic modules: MFM and STM. This hybrid design enables the model to effectively reconcile short-term fidelity with long-term coherence for streaming video understanding.

ritmic perception (Fechner, 1860; Scheler, 2017) for temporal organization and memory consolidation (Dudai, 2004; Buzsáki, 2021) for information refinement. Neuroscience research (Scheler, 2017) indicates that human brain encodes time on a non-uniform, logarithmic scale, preserving immediate stimuli with high fidelity while progressively distilling the distant past into a semantic “gist”. This suggests that a non-uniform temporal representation is fundamental for managing both local detail and global context. Complementing this, Neuroscience evidence (Buzsáki, 2021) reveals that the brain undergoes memory consolidation via mechanisms such as Sharp-Wave Ripples (SWRs), where extensive experiences are condensed into concise space thumbnails. This rapid replay and distillation process ensures the stability of long-term semantic structures. By emulating these dual principles, a streaming model can theoretically enable a more adaptive approach to maintaining continuous representations over extended horizons.

To translate these biological insights into a deployable architecture, we propose **FreshMem**, a **Frequency-Space Hybrid Memory** network. To embody logarithmic perception, we introduce the Multi-scale Frequency Memory (MFM) module. Rather than the uniform discarding prevalent in existing models, MFM utilizes Discrete Fourier Transforms (DFT) to project historical frames overflowing the sliding window (Xu et al., 2025b) into representative frequency coefficients. By using the superposition of these frequencies, MFM reconstructs the global “gist” of past context with minimal overhead, mitigating the raw data redundancy de-

scribed earlier. Parallelly, the memory consolidation mechanism is materialized through a Space Thumbnail Memory (STM) module. By monitoring episodic boundaries via cosine similarity, STM discretizes the continuous stream into distinct episodic clusters. An adaptive compression strategy then transforms these clusters into high-density space thumbnails, utilizing a centroid-based fusion mechanism to merge episodes with high semantic affinity.

To validate the effectiveness of the proposed FreshMem, we conduct extensive evaluations across both online streaming and offline video understanding benchmarks. In streaming scenarios, FreshMem delivers substantial performance gains over the competitive Qwen2-VL (Wang et al., 2024) baseline, achieving absolute accuracy improvements of 5.20% on StreamingBench (Lin et al., 2024), 4.52% on OV-Bench (Huang et al., 2025), and 2.34% on OVO-Bench (Niu et al., 2025). Remarkably, our training-free approach even outperforms several fully fine-tuned counterparts, underscoring its superior capacity for handling continuous data streams. Beyond streaming tasks, FreshMem also maintains robust performance on traditional offline benchmarks, yielding consistent improvements on the long-video benchmark MLVU (Zhou et al., 2025) and the short-video benchmark MVBench (Li et al., 2024b). Overall, these results demonstrate that, as a training-free framework, FreshMem effectively reconciles short-term fidelity with long-term coherence, offering a highly efficient and scalable alternative to computationally intensive training paradigms. The main contributions of our work are summarized as follows:

Brain-inspired paradigm for streaming video. We bridge the gap between biological memory mechanisms and streaming MLLMs by mimicking the human brain’s logarithmic perception and memory consolidation. This novel perspective effectively addresses the structural dilemma between maintaining short-term fidelity and ensuring long-term semantic coherence in continuous video streams.

Frequency-Space Hybrid Memory Network. We propose FreshMem, a unified framework comprising two core components: the MFM module, which projects overflowing frames into representative frequency coefficients complemented by salient residuals to reconstruct the global “gist” of historical context; and the STM module, which discretizes continuous streams into episodic clusters and employs an adaptive compression strategy to distill them into high-density space thumbnails.

Training-free efficiency with SOTA performance. As a training-free, plug-and-play module, FreshMem can be seamlessly integrated into existing MLLMs. Extensive experiments show that it not only significantly boosts the performance of baselines across multiple streaming benchmarks but remarkably outperforms several fully fine-tuned methods, demonstrating superior efficacy and efficiency.

2. Related Work

2.1. Input-level Modulation for Video Understanding

In the context of long-form video, static downsampling remains the dominant paradigm. Methods like AKS (Tang et al., 2025), and BOLT (Liu et al., 2025) employ heuristic metrics or learnable policies to filter redundant frames based on query relevance, while TimeViper (Xu et al., 2025a) adopts linear-complexity architectures to process denser inputs efficiently. In dynamic streaming scenarios, modulation strategies shift toward managing a sliding computational window. TimeChat (Ren et al., 2024) attends time information by a time-aware frame encoder and a sliding window Q-Former, while StreamingAssistant (Jin et al., 2025) further reduce redundancy by pruning tokens based on spatial adjacency or decoupling positional encodings.

Current methods, limited by rigid spatial heuristics and uniform windowing, overlook temporal nuances. Consequently, they sacrifice high-frequency details like subtle motion, hindering the reconciliation of local fidelity with the evolving narrative.

2.2. Memory-augmented Architectures for Video Understanding

A primary direction involves KV cache compression. LiveVLM (Ning et al., 2025) and InfiniPot-V (Kim et al., 2025) dynamically prune redundant key-value pairs in the

streaming cache. Another direction focuses on global token condensation and external banks. Pioneering works like MovieChat (Song et al., 2024) and MA-LMM (He et al., 2024) condense history into token-based summaries. More recent frameworks enforce structure upon these memories: Dispider (Qian et al., 2025) features a lightweight proactive streaming video processing module to determine the use of memory, and Flash-VStream (Zhang et al., 2024a) employs dual-layer storage. Furthermore, VideoLLaMB (Wang et al., 2025) introduces recurrent bridges to smooth transitions.

Current architectures fail to capture continuous temporal dynamics, often yielding fragmented representations caused by heavy spatial or lossy textual dependencies. Our proposed FreshMem overcomes this by balancing the retention of critical long-term information with short-term sensitivity, ensuring robust long-horizon reasoning.

3. FreshMem

3.1. Theory Foundations

FreshMem is grounded in two fundamental neuroscientific observations regarding temporal perception and episodic replay: the Weber-Fechner Law (Fechner, 1860) of logarithmic perception (Scheler, 2017) and the Sharp-Wave Ripples (SWRs) (Buzsáki, 2021) mechanism for memory consolidation (Dudai, 2004).

Weber-Fechner Law. Research in psychophysics suggests that the brain’s perception of time is non-uniform (Scheler, 2017). According to the Weber-Fechner Law, the relationship between the objective magnitude of a physical stimulus and its subjective perception is logarithmic rather than linear (Jeans, 1968).

Formally, let Δt be the time interval from the current moment. The perceived information density $I(\Delta t)$ can be modeled as:

$$I(\Delta t) \propto \frac{1}{k \cdot \ln(\Delta t + \epsilon)} \quad (1)$$

where k is a scaling constant and ϵ prevents singularity. This biological prior motivates us to project historical context into a domain where information density naturally decays, rather than storing frames with uniform density.

Sharp-Wave Ripples (SWRs). While the Weber-Fechner law describes passive decay, the brain also employs active consolidation mechanisms. During slow-wave sleep or rest, the hippocampus generates Sharp-Wave Ripples (SWRs). These high-frequency oscillations support the “fast replay” of sequential experiences, compressing long continuous episodes into brief, high-density neural bursts (Buzsáki, 2021).

Mathematically, we model this biological process as a Space Compression Operator Ψ . Given a continuous stream of vi-

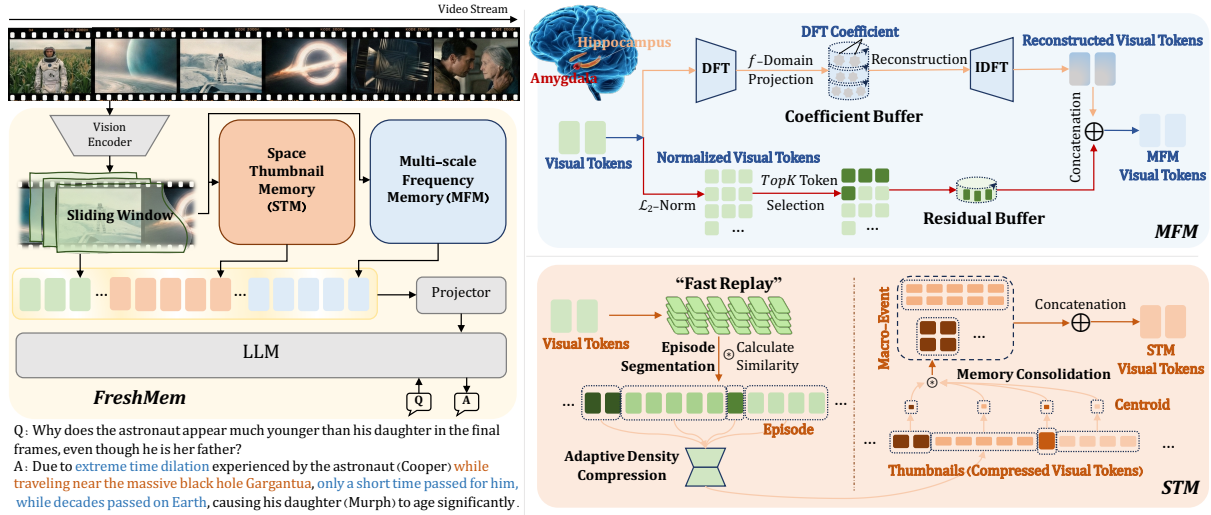


Figure 2. Illustration of FreshMem. (1) Sliding window for immediate high-fidelity context; (2) MFM, which maintains a global history by frequency coefficients and salient residuals; and (3) STM, which performs online episode segmentation and adaptive compression to keep key spatial thumbnails. The concatenated memory features enable the LLM to answer long-horizon queries with high accuracy.

sual features $E = \{x_1, x_2, \dots, x_T\}$ representing an episode, the SWRs mechanism functions as a non-linear integration that maps the sequence to a high-density “memory trace” \mathbf{m} :

$$\mathbf{m} = \Psi(E) \approx \frac{1}{|E|} \sum_{i=1}^T \mathbb{I}(x_i) \cdot x_i \quad (2)$$

where $\mathbb{I}(\cdot)$ denotes a saliency filter. This implies that extensive space redundancy is removed, retaining only the topological “centroid” of the event. This inspires our strategy of dynamically monitoring semantic boundaries to fuse redundant frames into “episodic clusters”, preserving topology within a limited budget.

3.2. Frequency-Space Hybrid Memory Network

Guided by these principles, we propose the FreshMem framework. As illustrated in the left of Figure 2, video frames are processed by a vision encoder and buffered in a sliding window \mathcal{M}_{short} for immediate context. To retain long-term information, overflowed frames are parallelly assimilated by Multi-scale Frequency Memory (MFM) for global “gist” reconstruction and Space Thumbnail Memory (STM) for episodic clustering. Finally, tokens from these memories are aggregated via a projector and fed into the LLM, enabling robust long-horizon streaming reasoning.

3.2.1. MULTI-SCALE FREQUENCY MEMORY (MFM)

To balance immediate precision with long-term retention, MFM operates in conjunction with sliding window that stores raw features of the most recent frames. As frames overflow, they are not discarded but projected into the frequency domain.

Incremental Frequency Update. Standard DFT requires access to the entire history, which is infeasible for streaming. We implement a recurrent update mechanism. Let $C_t \in \mathbb{C}^{K \times D}$ denote the frequency coefficients at step t , where K is the number of frequency bands. For an incoming overflowed frame x_t , we update the coefficients incrementally:

$$C_t[k] = \gamma \cdot C_{t-1}[k] + x_t \cdot e^{-j\omega_k t} \quad (3)$$

where ω_k is the angular frequency derived from the Weber-Fechner scale, and $\gamma \in (0, 1)$ is a decay factor preventing saturation. This ensures $O(1)$ update complexity. The coefficients are stored in a circular buffer structure; when the buffer is full, the pointer wraps around, overwriting the oldest frequency interactions, naturally mimicking the fading of very distant memories (Murre & Dros, 2015).

Amygdala-Inspired Residuals. Biological memory is not purely semantic; the *Amygdala* ensures that emotionally salient or shocking events are retained with high fidelity (LeDoux, 2007), regardless of their frequency characteristics. Inspired by this, and leveraging observations in (Tenney et al., 2019) that feature magnitude correlates with information importance, we introduce a *salient residual mechanism*.

During the update, we calculate the L_2 -norm of the input feature $\|x_t\|_2$ as a proxy for information entropy denoted as $\mathcal{B}_{residual}$. We retain the top- k elements with the highest norm as residual tokens \mathbf{r}_t :

$$\mathbf{r}_t = \begin{cases} x_t, & \text{if } \|x_t\|_2 \in \text{TopK}(\mathcal{B}_{residual}) \\ \mathbf{0}, & \text{otherwise} \end{cases} \quad (4)$$

Table 1. Evaluation results on OV-Bench. FP, THV, PM, SP, STP, TP **Table 2. Evaluation on OVO-Bench.** RTVP, BT, FAR denote represent Future Prediction, Temporal Hallucination Verification, Past Real-Time Visual Perception, Backward Tracing, Forward Active Memory, Spatial, Spatio-Temporal, Temporal Perception respectively.

Method	FP	THV	PM	SP	STP	TP	Avg.
<i>Proprietary MLLMs</i>							
Gemini-1.5-Flash (Team et al., 2024)	48.97	52.63	49.03	34.90	68.50	50.83	50.7
<i>Open-source Offline Video MLLMs</i>							
InternVL2-7B (Chen et al., 2024b)	46.80	56.00	54.73	34.70	62.20	37.57	48.7
InternVL2-4B (Chen et al., 2024b)	43.03	56.20	46.13	25.50	57.65	34.50	44.1
LLaMA-VID-7B (Li et al., 2024c)	38.03	52.77	43.17	21.55	50.25	41.70	41.9
LLaVA-Onevision-7B (Li et al., 2024a)	55.53	51.73	49.37	28.65	68.10	43.00	49.5
LongVA-7B (Zhang et al., 2024b)	50.03	47.20	49.53	17.50	56.05	36.90	43.6
MiniCPM-V2.6-7B (Yao et al., 2024)	28.07	55.03	34.70	19.20	67.30	32.90	39.1
LITA-7B (Huang et al., 2024b)	21.20	38.20	12.27	10.75	29.55	10.43	20.4
TimeChat-7B (Ren et al., 2024)	13.90	16.00	11.20	13.50	12.10	10.07	12.8
VTimeLLM-7B (Huang et al., 2024a)	25.20	53.93	32.40	23.15	23.85	33.50	33.1
<i>Open-source Online Video MLLMs</i>							
VideoLLM-Online-7B (Chen et al., 2024a)	7.57	14.57	9.67	13.60	10.40	3.63	9.6
MovieChat-7B (Song et al., 2024)	24.73	47.53	26.87	33.25	26.65	25.57	30.9
Flash-Vstream-7B (Zhang et al., 2024a)	29.47	47.33	28.27	26.75	24.20	27.40	31.2
InternVL2-2B (Chen et al., 2024b)	44.36	49.66	50.24	23.64	52.72	26.44	42.06
+FreshMem	46.62	54.13	59.69	30.64	57.79	29.76	47.44(5.38%)
Qwen2VL-7B (Wang et al., 2024)	45.39	50.47	57.80	22.71	69.02	30.66	46.30
+FreshMem	50.38	59.73	60.87	25.51	72.64	32.39	50.82(4.52%)

This dual-pathway storage mimics the Hippocampus’ global low-frequency context and Amygdala’s sparse high-frequency saliency collaboration (Richter-Levin & Akirav, 2000).

Holographic Reconstruction. During retrieval at step τ , we reconstruct the history \hat{H} by performing the Inverse Discrete Fourier Transform (IDFT) on the frequency coefficients and fusing them with the retrieved residuals:

$$\hat{H}_\tau = \text{Real} \left(\sum_{k=1}^K C_t[k] \cdot e^{j\omega_k \tau} \right) \oplus \mathbf{r}_\tau \quad (5)$$

This reconstruction allows the model to “hallucinate” the gist of the entire history while preserving sharp details for key frames.

3.2.2. SPACE THUMBNAIL MEMORY (STM)

While MFM handles global context, STM is designed to discretize continuous streams into structured “episodic clusters”, capturing the topological evolution of events.

Episode Segmentation. Similar to MFM, frames first pass through sliding window. Upon eviction, STM monitors the semantic continuity. We define an episode boundary based on the cosine similarity between the current frame x_t and the preceding context x_{t-1} :

$$\delta(t) = \frac{x_t \cdot x_{t-1}}{|x_t| |x_{t-1}|} < \theta_{event} \quad (6)$$

If the similarity score $\delta(t)$ drops below the threshold θ_{event} , a new episodic cluster E_{new} is initialized; otherwise, x_t is appended to the current active episode.

Adaptive Density Compression. Within each episode, we apply an adaptive compression strategy to maintain a

Method	RTVP	BT	FAR	Avg.
<i>Proprietary MLLMs</i>				
Gemini 1.5 Pro (Team et al., 2024)	69.32	62.54	57.15	63.00
GPT-4o (Hurst et al., 2024)	64.46	60.75	53.40	59.54
<i>Open-source Offline Video MLLMs</i>				
LLaVA-Video (Zhang et al., 2024c)	63.34	41.68	54.17	53.06
LLaVA-OneVision (Li et al., 2024a)	62.79	44.99	50.85	52.88
InternVL2-8B (Chen et al., 2024b)	60.73	44.00	45.42	50.05
LongVU-7B (Shen et al., 2024)	57.40	39.49	48.54	48.48
<i>Open-source Online Video MLLMs</i>				
VideoLLM-online (Chen et al., 2024a)	20.79	17.73	-	12.84
Flash-VStream (Zhang et al., 2024a)	29.86	25.35	44.23	33.15
Dispider-7B (Qian et al., 2025)	54.55	36.06	34.72	41.78
InternVL2-2B (Chen et al., 2024b)	44.92	34.55	41.93	41.22
+FreshMem	47.79	40.10	42.63	43.53(2.31%)
Qwen2VL-7B (Wang et al., 2024)	60.65	49.13	48.86	52.19
+FreshMem	66.67	54.04	48.25	54.53(2.34%)

constant “information density”. The sampling rate ρ is dynamically adjusted based on the episode duration N . For an episode E_i with N frames, the stored representation \mathbf{Z}_i is obtained by adaptive downsampling:

$$\mathbf{Z}_i = \text{Sample}(E_i, \rho(N)) \quad (7)$$

where the sampling rate $\rho(N) \propto \text{clamp}(N, \rho_{min}, \rho_{max})$ adapts to the episode length. This ensures that short, fast-paced actions retain higher frame rates, while long, redundant stationary scenes are heavily compressed, optimizing the storage budget.

Centroid-based Memory Consolidation. To strictly enforce the memory budget, we propose a topology-aware merge strategy. Instead of simply discarding the oldest event (FIFO), we calculate the *semantic centroid* μ_i for each stored episode E_i . When the memory is full, we compute the pairwise similarity S_{merge} between adjacent event centroids:

$$S_{merge}(i, i+1) = \frac{\mu_i \cdot \mu_{i+1}}{|\mu_i| |\mu_{i+1}|} \quad (8)$$

If S_{merge} exceeds the fusion threshold θ_{merge} , the two episodes are merged into a single “Macro-Event”, summing their frame counts and re-calculating the unified centroid. This mechanism effectively fuses redundant micro-events into a coherent narrative, preserving the deep semantic topology of the video.

3.2.3. GLOBAL MEMORY INTEGRATION

Finally, the comprehensive memory representation \mathcal{M}_{total} for the FreshMem framework is constructed by concatenating the outputs of all three modules:

$$\mathcal{M}_{total} = [\mathcal{M}_{MFM} \parallel \mathcal{M}_{STM} \parallel \mathcal{M}_{short}] \quad (9)$$

Table 3. Evaluation results on StreamingBench.

Method	OP	CR	CS	ATP	EU	TR	PR	SU	ACP	CT	ALL
<i>Proprietary MLLMs</i>											
Gemini 1.5 Pro (Team et al., 2024)	79.02	80.47	83.54	79.67	80.00	84.74	77.78	64.23	71.95	48.70	75.69
GPT-4o (Hurst et al., 2024)	77.11	80.47	83.91	76.47	70.19	83.80	66.67	62.19	69.12	49.22	73.28
Claude 3.5 Sonnet (Anthropic, 2024)	73.33	80.47	84.09	82.02	75.39	79.53	61.11	61.79	69.32	43.09	72.44
<i>Open-source Offline Video MLLMs</i>											
Video-LLaMA2-7B (Cheng et al., 2024)	55.86	55.47	57.41	58.17	52.80	43.61	39.81	42.68	45.61	35.23	49.52
LongVA-7B (Zhang et al., 2024b)	70.03	63.28	61.20	70.92	62.73	59.50	61.11	53.66	54.67	34.72	59.96
InternVL2-8B (Chen et al., 2024b)	68.12	60.94	69.40	77.12	67.70	62.93	59.26	53.25	54.96	56.48	63.72
Kangaroo-7B (Liu et al., 2024)	71.12	84.38	70.66	73.20	67.08	61.68	56.48	55.69	62.04	38.86	64.60
LLaVA-NeXT-Video-32B (Zhang et al., 2024c)	78.20	70.31	73.82	76.80	63.35	69.78	57.41	56.10	64.31	38.86	66.96
MiniCPM-V2.6-8B (Yao et al., 2024)	71.93	71.09	77.92	75.82	64.60	65.73	70.37	56.10	62.32	53.37	67.44
LLaVA-OneVision-7B (Li et al., 2024a)	80.38	74.22	76.03	80.72	72.67	71.65	67.59	65.45	65.72	45.08	71.12
Qwen2.5-VL-7B (Bai et al., 2025)	78.32	80.47	78.86	80.45	76.73	78.50	79.63	63.41	66.19	53.19	73.68
<i>Open-source Online Video MLLMs</i>											
Flash-VStream-7B (Zhang et al., 2024a)	25.89	43.57	24.91	23.87	27.33	13.08	18.52	25.20	23.87	48.70	23.23
VideoLLM-online-8B (Chen et al., 2024a)	39.07	40.06	34.49	31.05	45.96	32.40	31.48	34.16	42.49	27.89	35.99
Dispider-7B (Qian et al., 2025)	74.92	75.53	74.10	73.08	74.44	59.92	76.14	62.91	62.16	45.80	67.63
ReKV-7B (Di et al., 2025)	74.39	78.91	78.55	77.12	68.32	67.91	67.59	62.60	64.31	44.56	69.08
LiveVLM-7B (Ning et al., 2025)	81.47	78.13	83.28	79.08	69.57	74.14	75.00	69.11	67.71	40.41	72.92
InternVL2-2B (Chen et al., 2024b)	58.58	50.78	59.62	66.89	57.50	49.22	52.78	48.37	47.31	18.13	52.08
+FreshMem	64.85	57.81	66.56	72.46	63.75	58.26	60.19	52.44	53.82	19.17	58.21(↑ 6.13%)
Qwen2VL-7B (Wang et al., 2024)	77.38	76.56	73.19	75.08	75.00	67.91	73.15	65.04	66.57	35.75	69.00
+FreshMem	84.47	83.59	77.60	83.28	78.12	80.37	70.37	74.39	66.86	30.05	74.20(↑ 5.20%)

This hybrid token sequence provides the downstream predictor with global historical context, structured episodic summaries and immediate details.

4. Experiments

We employ Qwen2-VL-7B (Wang et al., 2024) and InternVL2-2B (Chen et al., 2024b) as baselines and test the performance on both online benchmarks (see Section 4.1) and offline benchmarks (see Section 4.2). FreshMem is training-free and it can be directly applied on top of baseline video MLLMs during inference. All experiments are conducted on RTX4090 GPUs.

4.1. Online Benchmark Results

We evaluate the performance of our model on three benchmarks for online video question answering: OV-Bench (Huang et al., 2025), OVO-Bench (Niu et al., 2025), and StreamingBench (Lin et al., 2024). These benchmarks are formulated as multiple-choice questions. For each question, the answer must be generated solely based on the video content before the corresponding timestamp, without access to the entire video.

Experimental results of these three benchmarks are shown in Tables 1 to 3. FreshMem achieves stable and significant performance improvement over different baselines and benchmarks. Built upon Qwen2-VL-7B, it obtains an accuracy of 50.82% on OV-Bench, 54.53% on OVO-Bench, and 74.2% on StreamingBench, yielding absolute improvements of 4.52%, 2.34%, and 5.20% over the baseline, respectively. This improvement arises from FreshMem’s brain-inspired memory strategy, which retains recent details with a frequency domain projection while compressing long-term

context into semantic gist and episodic thumbnails. Notably, our method outperforms several supervised approaches, despite not requiring extensive training. By aligning memory retention with video temporal structure, our method preserves both short-term precision and long-term coherence without additional training.

4.2. Offline Benchmark Results

We further evaluate our method on one long video understanding benchmark MLVU (Zhou et al., 2025) and one short video benchmark MVBench (Li et al., 2024b) and report the results in Table 4. In these offline settings, the MLLM is given access to the complete video as input. Our method demonstrates improvement upon the Qwen2VL-7B baseline by 2.4% on MLVU and by 4.7% on MVBench. These results highlight that our method not only excels on online benchmarks but also generalizes effectively to offline benchmarks.

Table 4. Evaluation results on MLVU and MVBench.

Method	MLVU	MVBench
LongVA-7B (Zhang et al., 2024b)	56.3	-
LLaVA-OneVision-7B (Li et al., 2024a)	64.7	56.7
LLaVA-Video-7B (Zhang et al., 2024c)	70.8	58.6
MovieChat-7B (Song et al., 2024)	-	55.1
Qwen2VL-7B (Wang et al., 2024)	54.9	59.1
+FreshMem	57.3(↑ 2.4%)	63.8(↑ 4.7%)

4.3. Visualization and Case Study

To enhance the interpretability of FreshMem, we visualized the reconstructed visual tokens during the streaming video process by decoding them back into complete video frames, as illustrated in Figure 4. As observed in the fig-

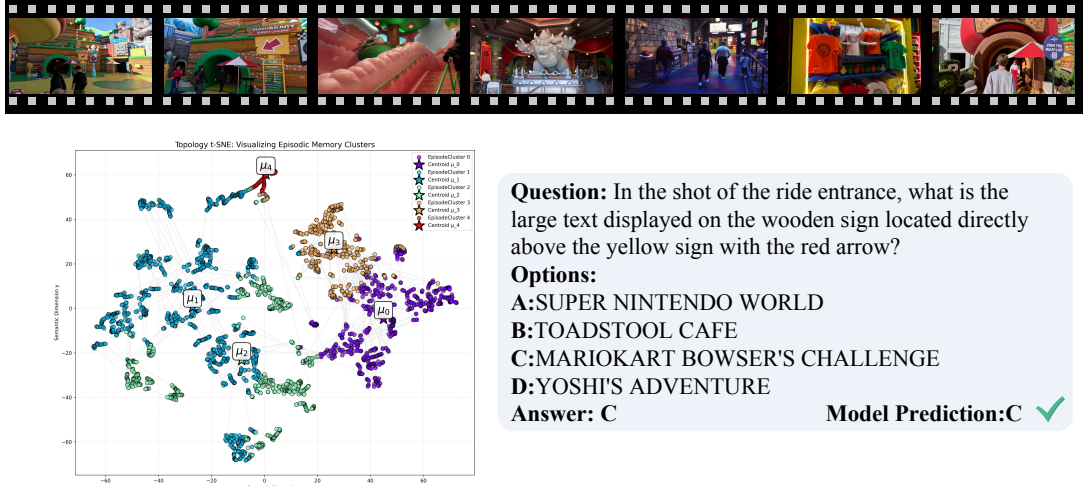


Figure 3. Interpretability analysis of the STM module. The t-SNE visualization illustrates the effectiveness of our Memory Consolidation mechanism, showing how continuous video streams are discretized into coherent episodic clusters.

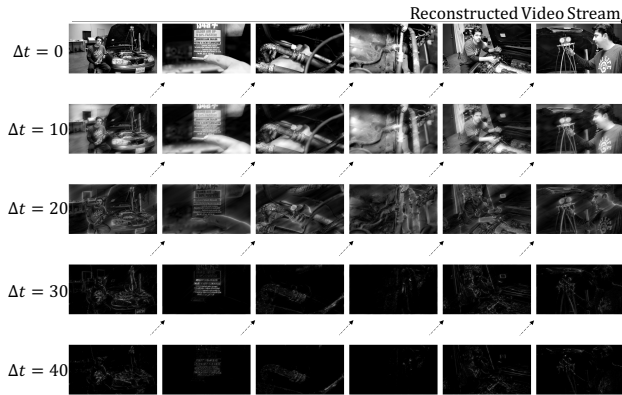


Figure 4. Reconstructed video stream from frequency coefficients. The visualization demonstrates the information decay inherent in our MFM module.

ure, frames further from the current timestamp (Δt) appear increasingly blurred and tend towards a binary-like representation. This demonstrates that following DFT and IDFT processing, the MFM effectively preserves the “gist” information—maintaining a rough outline of past events that gradually decays over time. This phenomenon empirically validates the rationality of the logarithmic perception mechanism inherent in our MFM module.

Furthermore, we visualized the reconstruction of the top- k residual tokens selected within the MFM, as shown in Figure 5. The visualization reveals that the selected top- k tokens are predominantly distributed along the edges of people and objects, clustering in semantically dense regions within each frame. This empirically validates that these residual tokens serve as a vital complement to the reconstructed visual

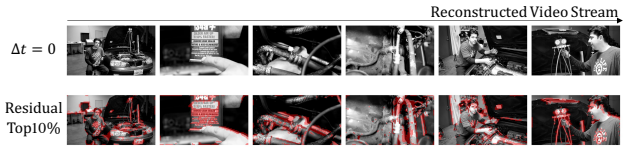


Figure 5. Impact of Salient Residual Tokens. We visualize the reconstruction of the top-10% residual tokens selected by the MFM.

tokens for timestamps distant from the present tend to fade into a blurred background, the residual tokens effectively delineate sharp contours and structural details on top of them. Together, these two components work synergistically to achieve robust memory and recall of past events.

Finally, we conduct an interpretability experiment and a case study specifically for the STM module, as illustrated in Figure 3. We visualized the “episode clusters” using t-SNE and annotated the centroid (μ) of each cluster. In conjunction with the provided case study, we can observe that although the streaming video contains frames that are semantically similar but temporally discontinuous, our proposed episode segmentation and cluster fusion mechanisms enable the model to effectively capture these underlying temporal correlations. This empirically validates that our STM module mimics the biological process of memory consolidation, effectively reducing the semantic fragmentation of visual information.

4.4. Ablation Studies

To evaluate the effectiveness of each component in our proposed method, we conduct a series of ablation experiments on the OVO-Bench. As shown in Table 5, the baseline Qwen2-VL-7B model achieves an average score of 52.19%.

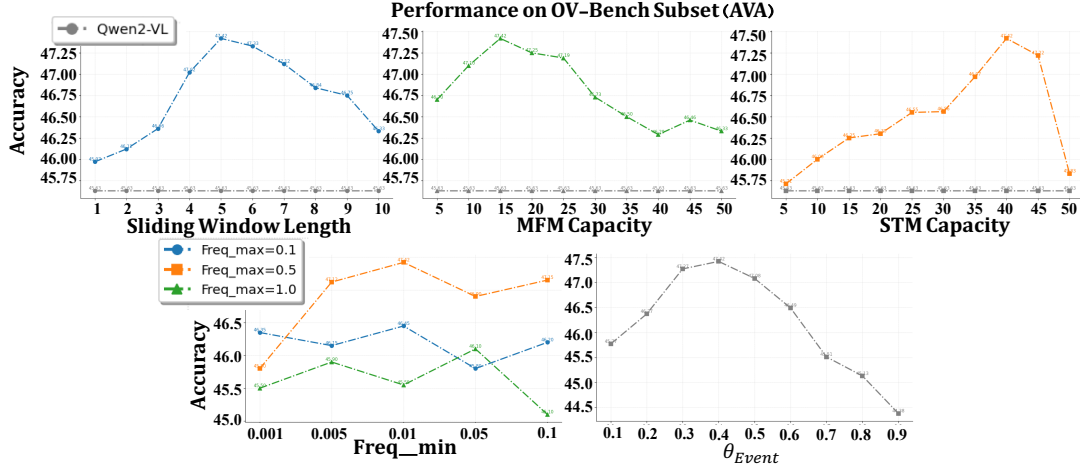


Figure 6. Sensitivity analysis of FreshMem hyperparameters. Experiments on the OV-Bench subset demonstrate the robustness of our default settings.

Table 5. Ablation study on OVO-Bench results. SW represents Sliding Window.

Model	SW	STM	MFM	Avg.
Qwen2-VL-7B	✗	✗	✗	52.19
+ SW	✓	✗	✗	52.52
+ STM	✗	✓	✗	53.64
+ MFM	✗	✗	✓	53.54
+ SW + STM	✓	✓	✗	53.92
+ SW + MFM	✓	✗	✓	54.36
+ STM + MFM	✗	✓	✓	54.05
Ours	✓	✓	✓	54.53

By individually integrating the Sliding Window (SW), STM, and MFM, we observe consistent performance gains of 0.33%, 1.45%, and 1.35% respectively, demonstrating the necessity of each module. Combining these components further boosts the performance, and our full configuration (SW + STM + MFM) achieves the best result of 54.53%, which is a 2.34% absolute improvement over the baseline.

To verify the impact of key hyperparameters and determine the optimal configuration, we conduct a series of experiments on the OV-Bench Subset (AVA). The results are illustrated in Figure 6, covering sliding window length, memory module capacities (MFM and STM), frequency band, and the episode segmentation threshold θ_{event} . As shown in the top-left of Figure 6, performance peaks when the sliding window length is set to approximately 5 frames. A shorter window fails to capture sufficient temporal context, while an excessively long window introduces redundancy or noise, leading to performance degradation. Then we analyzed the capacity settings for MFM and STM modules in the top-middle and top-right plots of Figure 6. For MFM, performance reaches optima at capacities of 15. For STM, accuracy improves with capacity, saturating and achieving near-optimal performance around a capacity of 40. Consider-

ing the trade-off between inference GPU memory usage, computational latency, and model accuracy, we prioritized efficiency.

The bottom-left plot in Figure 6 illustrates the model’s sensitivity to frequency band parameters ($Freq_min$ and $Freq_max$). The orange curve indicates that setting the high-frequency cutoff ($Freq_max$) to 0.5 yields the best overall performance. Furthermore, we observed that the model extracts the most discriminative temporal features when the high and low frequencies differ by approximately one order of magnitude.

Finally, we investigated the influence of the event update threshold, θ_{event} , within the STM module (Figure 6, bottom-right). This parameter controls the model’s sensitivity in distinguishing different episodes. The data shows that the model achieves a stable peak performance when θ_{event} is set between 0.3 and 0.4. Values outside this range resulted in a notable drop in accuracy. Detailed settings for all parameters are provided in Table 7.

5. Conclusion

In this paper, we proposed FreshMem, a brain-inspired framework that reconciles short-term fidelity with long-term coherence via frequency-domain projection and episodic clustering. Extensive experiments demonstrate that FreshMem achieves distinguished performance on multiple streaming benchmarks. Remarkably, despite being a training-free solution, it surpasses several fully fine-tuned methods, highlighting the superior efficacy of our structured memory design. These results suggest that integrating FreshMem into end-to-end training pipelines holds immense potential for unlocking even stronger long-horizon streaming video understanding capabilities.

Impact Statement

This paper presents work whose goal is to advance the field of Machine Learning. There are many potential societal consequences of our work, none of which we feel must be specifically highlighted here.

References

Achiam, J., Adler, S., Agarwal, S., Ahmad, L., Akkaya, I., Aleman, F. L., Almeida, D., Altenschmidt, J., Altman, S., Anadkat, S., et al. Gpt-4 technical report. *arXiv preprint arXiv:2303.08774*, 2023.

Anthropic. Claude 3.5 sonnet. Technical report, URL <https://www.anthropic.com/news/clause-3-5-sonnet>, 2024.

Bai, S., Chen, K., Liu, X., Wang, J., Ge, W., Song, S., Dang, K., Wang, P., Wang, S., Tang, J., et al. Qwen2.5-vl technical report. *arXiv preprint arXiv:2502.13923*, 2025.

Buzsáki, G. *The brain from inside out*. Oxford University Press, 2021.

Chatterjee, D., Remelli, E., Song, Y., Tekin, B., Mittal, A., Bhatnagar, B., Camgoz, N. C., Hampali, S., Sauser, E., Ma, S., et al. Streaming videollms for real-time procedural video understanding. In *Proceedings of the IEEE/CVF International Conference on Computer Vision*, pp. 22586–22598, 2025.

Chen, J., Lv, Z., Wu, S., Lin, K. Q., Song, C., Gao, D., Liu, J.-W., Gao, Z., Mao, D., and Shou, M. Z. Videollm-online: Online video large language model for streaming video. In *Proceedings of the IEEE/CVF Conference on Computer Vision and Pattern Recognition*, pp. 18407–18418, 2024a.

Chen, Z., Wang, W., Cao, Y., Liu, Y., Gao, Z., Cui, E., Zhu, J., Ye, S., Tian, H., Liu, Z., et al. Expanding performance boundaries of open-source multimodal models with model, data, and test-time scaling. *arXiv preprint arXiv:2412.05271*, 2024b.

Cheng, Z., Leng, S., Zhang, H., Xin, Y., Li, X., Chen, G., Zhu, Y., Zhang, W., Luo, Z., Zhao, D., et al. Videollama 2: Advancing spatial-temporal modeling and audio understanding in video-llms. *arXiv preprint arXiv:2406.07476*, 2024.

Di, S., Yu, Z., Zhang, G., Li, H., Cheng, H., Li, B., He, W., Shu, F., Jiang, H., et al. Streaming video question-answering with in-context video kv-cache retrieval. In *The Thirteenth International Conference on Learning Representations*, 2025.

Dudai, Y. The neurobiology of consolidations, or, how stable is the engram?. *Annual review of psychology* vol. 55 (2004): 51-86. doi:10.1146/annurev.psych.55.090902.142050, 2004.

Fechner, G. T. *Elements of psychophysics [Elemente der Psychophysik]*. Leipzig : Breitkopf und Härtel, 1860.

He, B., Li, H., Jang, Y. K., et al. Ma-lmm: Memory-augmented large multimodal model for long-term video understanding. In *Proceedings of the IEEE/CVF Conference on Computer Vision and Pattern Recognition (CVPR)*, pp. 13504–13514, 2024.

Huang, B., Wang, X., Chen, H., Song, Z., and Zhu, W. Vtimellm: Empower llm to grasp video moments. In *Proceedings of the IEEE/CVF Conference on Computer Vision and Pattern Recognition*, pp. 14271–14280, 2024a.

Huang, D.-A., Liao, S., Radhakrishnan, S., Yin, H., Molchanov, P., Yu, Z., and Kautz, J. Lita: Language instructed temporal-localization assistant. In *European Conference on Computer Vision*, pp. 202–218. Springer, 2024b.

Huang, Z., Li, X., Li, J., Wang, J., Zeng, X., Liang, C., Wu, T., Chen, X., Li, L., and Wang, L. Online video understanding: Ovbench and videochat-online. In *Proceedings of the Computer Vision and Pattern Recognition Conference*, pp. 3328–3338, 2025.

Hurst, A., Lerer, A., Goucher, A. P., Perelman, A., Ramesh, A., Clark, A., Ostrow, A., Welihinda, A., Hayes, A., Radford, A., et al. Gpt-4o system card. *arXiv preprint arXiv:2410.21276*, 2024.

Jeans, J. *Science & music*. New York : Dover Publications, 1968.

Jin, X., Yu, H., Yu, B., et al. Streamingassistant: Efficient visual token pruning for accelerating online video understanding. *arXiv preprint arXiv:2512.12560*, 2025.

Kim, M., Shim, K., Choi, J., et al. Infinipot-v: Memory-constrained kv cache compression for streaming video understanding. *arXiv preprint arXiv:2506.15745*, 2025.

LeDoux, J. The amygdala. *Current biology*, 17(20):R868–R874, 2007.

Li, B., Zhang, Y., Guo, D., Zhang, R., Li, F., Zhang, H., Zhang, K., Zhang, P., Li, Y., Liu, Z., et al. Llava-onevision: Easy visual task transfer. *arXiv preprint arXiv:2408.03326*, 2024a.

Li, K., Wang, Y., He, Y., Li, Y., Wang, Y., Liu, Y., Wang, Z., Xu, J., Chen, G., Luo, P., et al. Mvbench: A comprehensive multi-modal video understanding benchmark. In

Proceedings of the IEEE/CVF Conference on Computer Vision and Pattern Recognition, pp. 22195–22206, 2024b.

Li, Y., Wang, C., and Jia, J. Llama-vid: An image is worth 2 tokens in large language models. In *European Conference on Computer Vision*, pp. 323–340. Springer, 2024c.

Lin, J., Fang, Z., Chen, C., Wan, Z., Luo, F., Li, P., Liu, Y., and Sun, M. Streamingbench: Assessing the gap for mllms to achieve streaming video understanding. *arXiv preprint arXiv:2411.03628*, 2024.

Liu, J., Wang, Y., Ma, H., Wu, X., Ma, X., Wei, X., Jiao, J., Wu, E., and Hu, J. Kangaroo: A powerful video-language model supporting long-context video input. *arXiv preprint arXiv:2408.15542*, 2024.

Liu, S., Zhao, C., Xu, T., et al. Bolt: Boost large vision-language model without training for long-form video understanding. In *Proceedings of the IEEE/CVF Conference on Computer Vision and Pattern Recognition (CVPR)*, pp. 3318–3327, 2025.

Murre, J. M. and Dros, J. Replication and analysis of ebbinghaus' forgetting curve. *PloS one*, 10(7):e0120644, 2015.

Ning, Z., Liu, G., Jin, Q., Ding, W., Guo, M., and Zhao, J. Livevlm: Efficient online video understanding via streaming-oriented kv cache and retrieval. *arXiv preprint arXiv:2505.15269*, 2025.

Niu, J., Li, Y., Miao, Z., Ge, C., Zhou, Y., He, Q., Dong, X., Duan, H., Ding, S., Qian, R., et al. Ovo-bench: How far is your video-llms from real-world online video understanding? In *Proceedings of the Computer Vision and Pattern Recognition Conference*, pp. 18902–18913, 2025.

Qian, R., Dong, X., Zhang, P., Zang, Y., Ding, S., Lin, D., and Wang, J. Streaming long video understanding with large language models. *Advances in Neural Information Processing Systems*, 37:119336–119360, 2024.

Qian, R., Ding, S., Dong, X., Zhang, P., Zang, Y., Cao, Y., Lin, D., and Wang, J. Dispider: Enabling video llms with active real-time interaction via disentangled perception, decision, and reaction. In *Proceedings of the Computer Vision and Pattern Recognition Conference*, pp. 24045–24055, 2025.

Ren, S., Yao, L., Li, S., Sun, X., and Hou, L. Timechat: A time-sensitive multimodal large language model for long video understanding. In *Proceedings of the IEEE/CVF Conference on Computer Vision and Pattern Recognition*, pp. 14313–14323, 2024.

Richter-Levin, G. and Akirav, I. Amygdala-hippocampus dynamic interaction in relation to memory. *Molecular neurobiology*, 22(1):11–20, 2000.

Scheler, G. Logarithmic distributions prove that intrinsic learning is hebbian. *F1000Res*. 2017 Jul 25;6:1222. doi: 10.12688/f1000research.12130.2. PMID: 29071065; PMCID: PMC5639933., 2017.

Shen, X., Xiong, Y., Zhao, C., Wu, L., Chen, J., Zhu, C., Liu, Z., Xiao, F., Varadarajan, B., Bordes, F., et al. Longvu: Spatiotemporal adaptive compression for long video-language understanding. *arXiv preprint arXiv:2410.17434*, 2024.

Song, E., Chai, W., Wang, G., Zhang, Y., Zhou, H., Wu, F., Chi, H., Guo, X., Ye, T., Zhang, Y., et al. Moviechat: From dense token to sparse memory for long video understanding. In *Proceedings of the IEEE/CVF Conference on Computer Vision and Pattern Recognition*, pp. 18221–18232, 2024.

Tang, X., Qiu, J., Xie, L., et al. Adaptive keyframe sampling for long video understanding. In *Proceedings of the IEEE/CVF Conference on Computer Vision and Pattern Recognition (CVPR)*, pp. 29118–29128, 2025.

Team, G., Georgiev, P., Lei, V. I., Burnell, R., Bai, L., Gulati, A., Tanzer, G., Vincent, D., Pan, Z., Wang, S., and et al. Gemini 1.5: Unlocking multimodal understanding across millions of tokens of context, 2024. URL <https://arxiv.org/abs/2403.05530>.

Tenney, I., Das, D., and Pavlick, E. Bert rediscovers the classical nlp pipeline. *arXiv preprint arXiv:1905.05950*, 2019.

Wang, P., Bai, S., Tan, S., Wang, S., Fan, Z., Bai, J., Chen, K., Liu, X., Wang, J., Ge, W., et al. Qwen2-vl: Enhancing vision-language model's perception of the world at any resolution. *arXiv preprint arXiv:2409.12191*, 2024.

Wang, Y., Song, Y., Xie, C., et al. Videollamb: Long streaming video understanding with recurrent memory bridges. In *Proceedings of the IEEE/CVF International Conference on Computer Vision (ICCV)*, pp. 24170–24181, 2025.

Xiong, H., Yang, Z., Yu, J., Zhuge, Y., Zhang, L., Zhu, J., and Lu, H. Streaming video understanding and multi-round interaction with memory-enhanced knowledge. *arXiv preprint arXiv:2501.13468*, 2025.

Xu, B., Xiao, Z., Li, J., et al. Timeviper: A hybrid mamba-transformer vision-language model for efficient long video understanding. *arXiv preprint arXiv:2511.16595*, 2025a.

Xu, R., Xiao, G., Chen, Y., He, L., Peng, K., Lu, Y., and Han, S. Streamingvlm: Real-time understanding for infinite video streams. *arXiv preprint arXiv:2510.09608*, 2025b.

Yang, Z., Li, L., Lin, K., Wang, J., Lin, C.-C., Liu, Z., and Wang, L. The dawn of lmms: Preliminary explorations with gpt-4v (ision). *arXiv preprint arXiv:2309.17421*, 2023.

Yao, Y., Yu, T., Zhang, A., Wang, C., Cui, J., Zhu, H., Cai, T., Li, H., Zhao, W., He, Z., et al. Minicpm-v: A gpt-4v level mllm on your phone. *arXiv preprint arXiv:2408.01800*, 2024.

Zeng, X., Qiu, K., Zhang, Q., Li, X., Wang, J., Li, J., Yan, Z., Tian, K., Tian, M., Zhao, X., et al. Streamforest: Efficient online video understanding with persistent event memory. *arXiv preprint arXiv:2509.24871*, 2025.

Zhang, H., Wang, Y., Tang, Y., Liu, Y., Feng, J., Dai, J., and Jin, X. Flash-vstream: Memory-based real-time understanding for long video streams. *arXiv preprint arXiv:2406.08085*, 2024a.

Zhang, P., Zhang, K., Li, B., Zeng, G., Yang, J., Zhang, Y., Wang, Z., Tan, H., Li, C., and Liu, Z. Long context transfer from language to vision. *arXiv preprint arXiv:2406.16852*, 2024b.

Zhang, Y., Wu, J., Li, W., Li, B., Ma, Z., Liu, Z., and Li, C. Video instruction tuning with synthetic data. *arXiv preprint arXiv:2410.02713*, 2024c.

Zhou, J., Shu, Y., Zhao, B., Wu, B., Liang, Z., Xiao, S., Qin, M., Yang, X., Xiong, Y., Zhang, B., et al. Mlvu: Benchmarking multi-task long video understanding. In *Proceedings of the Computer Vision and Pattern Recognition Conference*, pp. 13691–13701, 2025.

A. Inference Efficiency and Memory Analysis

To quantitatively assess the computational and memory overhead introduced by our proposed FreshMem, we conducted rigorous inference time and memory usage measurements on the Qwen2-VL-7B model using the AVA subset from OV-Bench —a representative benchmark for streaming video understanding. Our evaluation focuses on absolute inference latency, peak GPU memory usage, and the corresponding performance gains. The results are summarized in Table 6.

Table 6. Inference Efficiency Analysis on OV-Bench (AVA Subset). Comparison of inference latency, peak GPU memory usage, and accuracy between the baseline and our proposed method. FreshMem achieves a significant performance boost (+1.79%) with a moderate and acceptable increase in computational overhead, ensuring deployment feasibility on consumer-grade GPUs (e.g., RTX 4090).

Method	Latency	GPU Mem.	Accuracy (%)
Qwen2-VL-7B	1h 21min	17GB	45.63
+ FreshMem (Ours)	1h 35min	20GB	47.42

Controlled Computational and Memory Overhead. Compared to the vanilla Qwen2-VL-7B baseline, FreshMem introduces a moderate and highly controlled increase in resource consumption. Specifically, the relative time overhead is approximately $\times 1.17$ (increasing from 81 mins to 95 mins), and the GPU memory usage sees a marginal increase of roughly 17.6% (from 17GB to 20GB). Crucially, the peak memory footprint of 20GB remains well within the capacity of standard consumer-grade GPUs (e.g., RTX 3090/4090), ensuring that our method maintains broad hardware accessibility and operational feasibility without requiring specialized high-end infrastructure.

Breakdown of Overhead Sources. The primary computational overhead in our method stems from the specific memory operations: the incremental Discrete Fourier Transform (DFT) updates in the MFM module and the centroid-based clustering in the STM module. However, these components are mathematically designed to be lightweight with near-linear complexity regarding the window size. By avoiding the heavy retraining of the entire model, FreshMem minimizes the computational burden typically associated with long-context adaptation.

Efficiency-Performance Trade-off. The marginal additional resource consumption is well justified by the substantial performance gains observed. While incurring only a slight overhead in latency and memory, FreshMem achieves a significant performance boost, improving accuracy from 45.63% to 47.42% (+1.79%). This highlights that our approach strikes a highly favorable balance between computational complexity and memory-enhanced modeling capability. For latency-sensitive streaming applications, FreshMem offers a high-yield upgrade path that significantly enhances long-horizon reasoning with negligible impact on system throughput.

Summary. FreshMem maintains operational feasibility with predictable computational costs. It integrates seamlessly with the base model, providing a superior performance-efficiency trade-off that makes it suitable for both research exploration and real-world deployment scenarios where resources are constrained but high performance is demanded.

B. Detailed Hyperparameter Settings

Table 7. Hyperparameter settings in our experiments.

Hyperparameter	Value
Sliding Window Length	5
MFM Capacity	15
STM Capacity	40
Number of Frequency Bands	16
Frequency Range	0.01 ~ 0.5
Decay Factor (γ)	0.9
Residual Tokens Ratio	Top 10%
Event Threshold (θ_{event})	0.4
Merge Threshold (θ_{merge})	0.3
Sampling Rate (ρ)	1/16 ~ 1/4

C. Detailed Experimental Performance

We present the full evaluation results on OVO-Bench and MLVU in Tables 8 and 9. Table 8 shows the full evaluation results on OVO-Bench with all 12 subtasks. FreshMem demonstrates significant improvements over the Qwen2VL-7B baseline and outperforms many offline and online video MLLMs. Improvement on a specific subtask is up to 11.45%. Table 9 shows the full evaluation results on MLVU with all 7 MCQA subtasks. FreshMem outperforms baseline by 2.4% overall and up to 8.7% on a specific subtask.

Table 8. Full Evaluation results on OVO-Bench.

Model	Real-Time Visual Perception							Backward Tracing				Forward Active Responding				Overall Avg.
	OCR	ACR	ATR	STU	FPD	OJR	Avg.	EPM	ASI	HLD	Avg.	REC	SSR	CRR	Avg.	
<i>Offline Video MLLMs</i>																
Gemini 1.5 Pro (Team et al., 2024)	85.91	66.97	79.31	58.43	63.37	61.96	69.32	58.59	76.35	52.64	62.54	35.53	74.24	61.67	57.15	63.00
GPT-4o (Hurst et al., 2024)	69.80	64.22	71.55	51.12	70.30	59.78	64.46	57.91	75.68	48.66	60.75	27.58	73.21	59.40	53.40	59.54
<i>Offline Video MLLMs</i>																
LLaVA-Video-7B (Zhang et al., 2024c)	69.80	59.63	66.38	50.56	72.28	61.41	63.34	51.18	64.19	9.68	41.68	34.10	67.57	60.83	54.17	53.06
LLaVA-OneVision-7B (Li et al., 2024a)	67.11	58.72	69.83	49.44	71.29	60.33	62.79	52.53	58.78	23.66	44.99	24.79	66.93	60.83	50.85	52.88
InternVL2-8B (Chen et al., 2024b)	68.46	58.72	68.97	44.94	67.33	55.98	60.73	43.10	61.49	27.41	44.00	25.79	57.55	52.92	45.42	50.05
LongVU-7B (Shen et al., 2024)	55.70	49.54	59.48	48.31	68.32	63.04	57.40	43.10	66.22	9.14	39.49	16.62	69.00	60.00	48.54	48.48
<i>Online Video MLLMs</i>																
VideoLLM-online-8B (Chen et al., 2024a)	8.05	23.85	12.07	14.04	45.54	21.20	20.79	22.22	18.80	12.18	17.73	-	-	-	-	12.84
Flash-VStream-7B (Zhang et al., 2024a)	25.50	32.11	29.31	33.71	29.70	28.80	29.86	36.36	33.78	5.91	25.35	5.44	67.25	60.00	44.23	33.15
Dispider-7B (Qian et al., 2025)	57.72	49.54	62.07	44.94	61.39	51.63	54.55	48.48	55.41	4.30	36.06	18.05	37.36	48.75	34.72	41.78
Qwen2VL-7B (Wang et al., 2024)	69.13	53.21	63.79	50.56	66.34	60.87	60.65	45.79	48.65	54.84	49.13	30.09	65.66	50.83	48.86	52.19
+FreshMem	77.18	60.55	70.69	56.74	63.37	70.65	66.67	57.24	56.76	46.77	54.04	23.93	72.66	55.00	48.25	54.53(↑ 2.34%)

Table 9. Full Evaluation results on MLVU.

Method	TR	AR	NQA	ER	PQA	AO	AC	AVG
MovieChat (Song et al., 2024)	18.7	10.3	23.3	15.1	16.0	17.1	15.0	16.5
MA-LMM (He et al., 2024)	44.0	23.1	13.3	30.2	14.0	18.6	13.3	22.4
LLaVa-OneVision-7B (Li et al., 2024a)	83.5	56.4	46.7	58.4	58.0	35.7	23.3	51.7
Qwen2VL-7B (Wang et al., 2024)	80.3	70.0	61.7	48.6	56.2	40.9	20.4	54.9
+FreshMem	83.0	73.5	72.4	53.1	53.6	43.6	16.5	57.3(↑ 2.4%)

D. More Visualization Results

Figures 7 to 10 show more video frames of the current streaming video reconstructed from the MFM modules based on different DFT coefficients at different steps. We can still observe that MFM is capable of retaining the gist information from the past history, which is consistent with our discussion in the main text. Figures 11 to 14 show more residual tokens reconstructed in the MFM module. From the results, it can be seen that the crucial residual information is basically concentrated in the semantic important areas, which is consistent with our main conclusion in the text. MFM can maintain the historical semantic outline while preserving high-fidelity visual information.

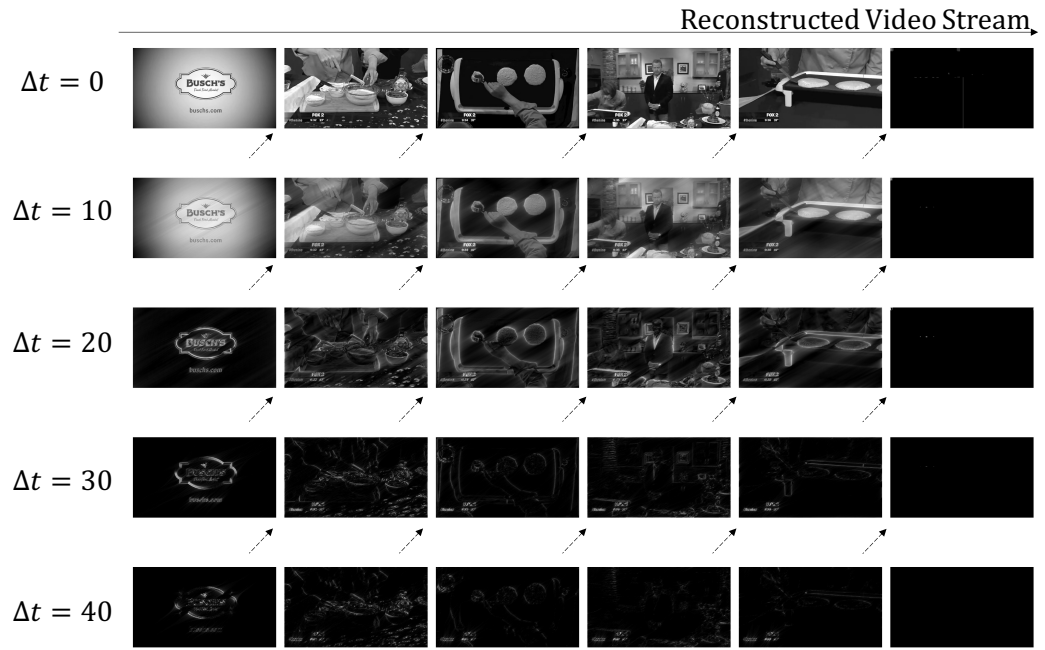


Figure 7. Reconstructed video stream from frequency coefficients.

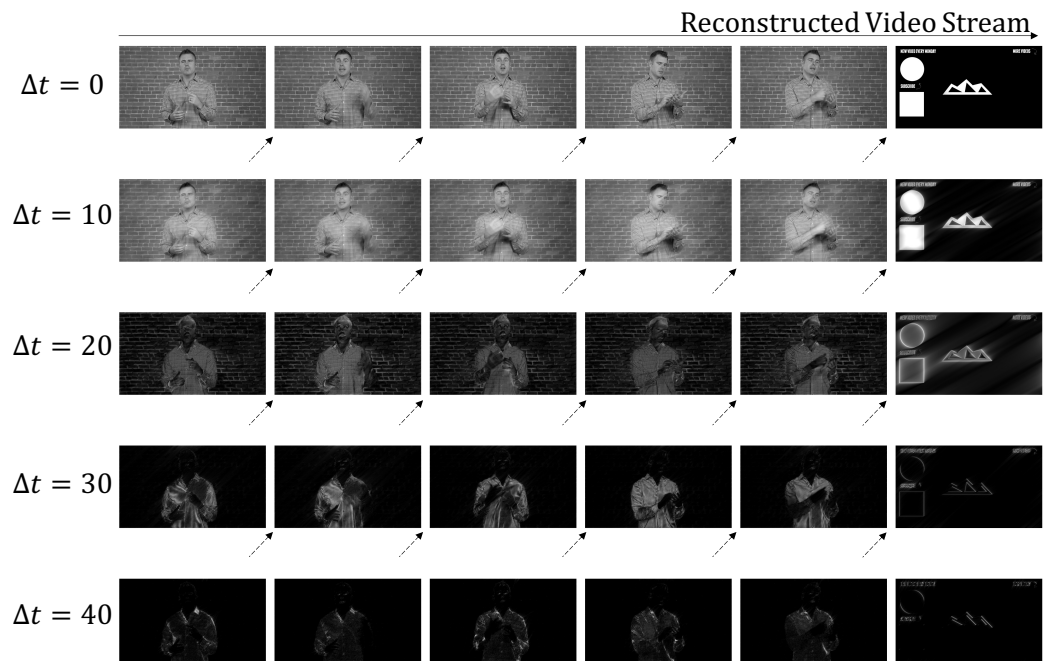


Figure 8. Reconstructed video stream from frequency coefficients.

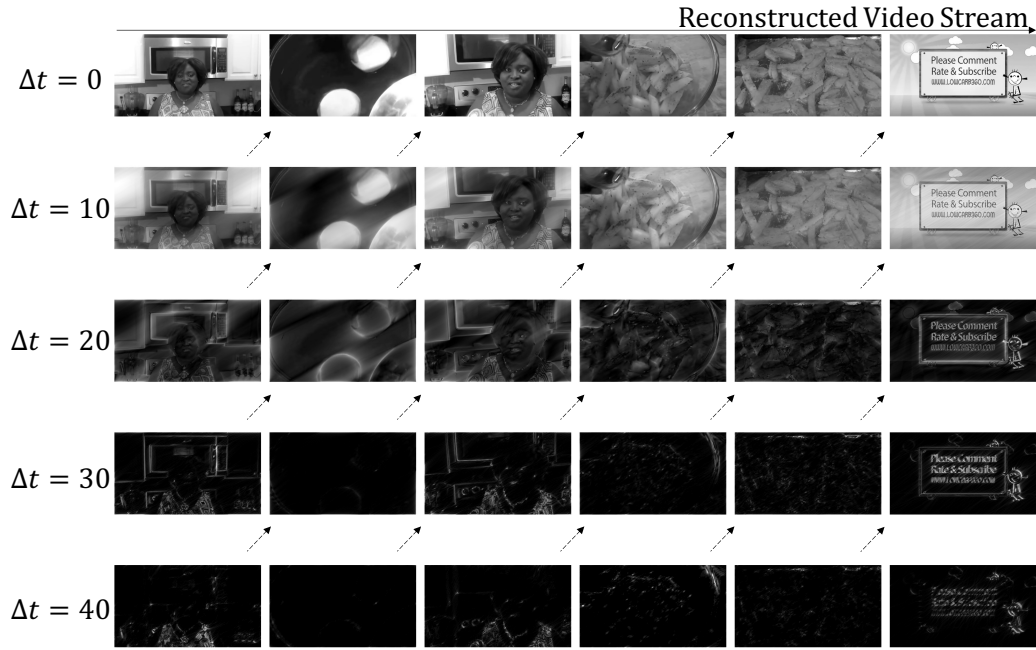


Figure 9. Reconstructed video stream from frequency coefficients.

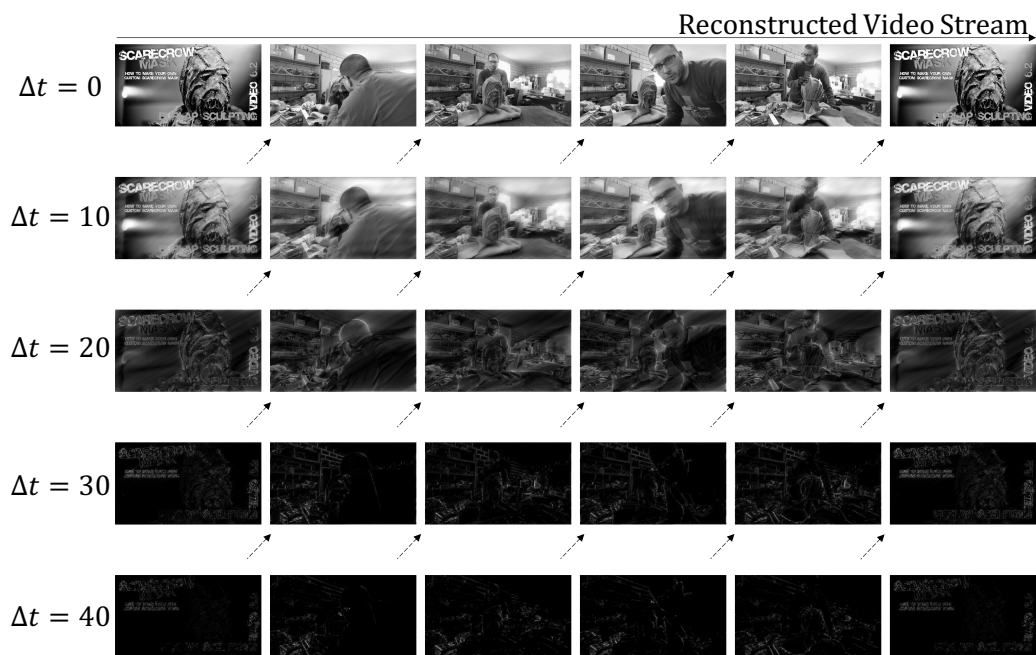


Figure 10. Reconstructed video stream from frequency coefficients.

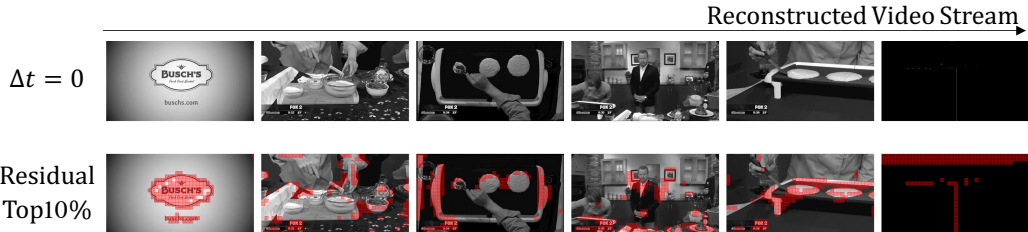


Figure 11. Impact of Salient Residual Tokens.

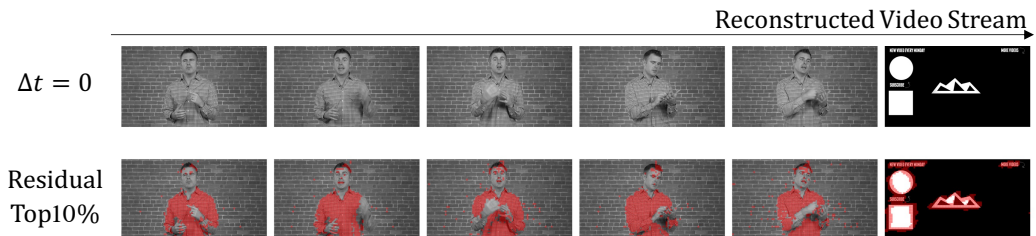


Figure 12. Impact of Salient Residual Tokens.

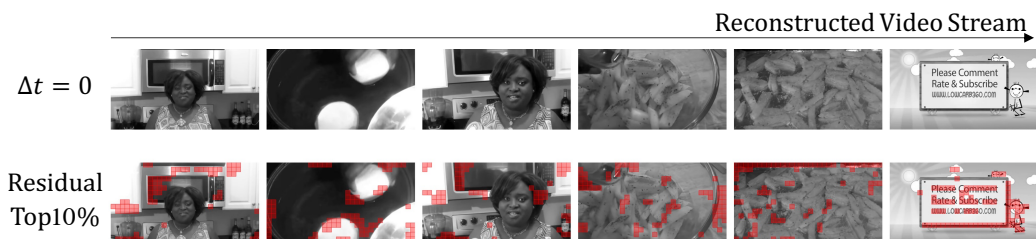
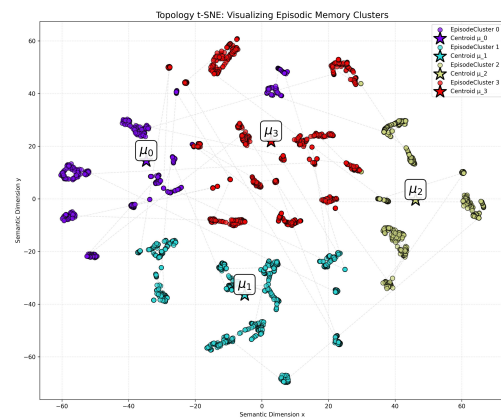


Figure 13. Impact of Salient Residual Tokens.



Figure 14. Impact of Salient Residual Tokens.

E. More Case Studies



Question: Early in the video, while walking through the produce section, the camera captured a man wearing a black jacket and sunglasses. What specific color of apples was he reaching for?

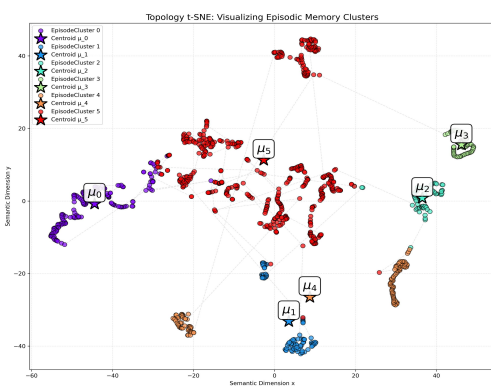
Options:

- A:Red
- B:Green
- C:Yellow
- D:He was reaching for oranges

Answer: B

Model Prediction: B ✓

Figure 15. Interpretability analysis of the STM module.



Question: After getting out of the car and walking towards the house, what object is the character (Mr. Bean) carrying in his hand?

Options:

- A:952R
- B:STE 952R
- C:SLW 287R
- D:BEAN 01

Answer: B

Model Prediction: B ✓

Figure 16. Interpretability analysis of the STM module.

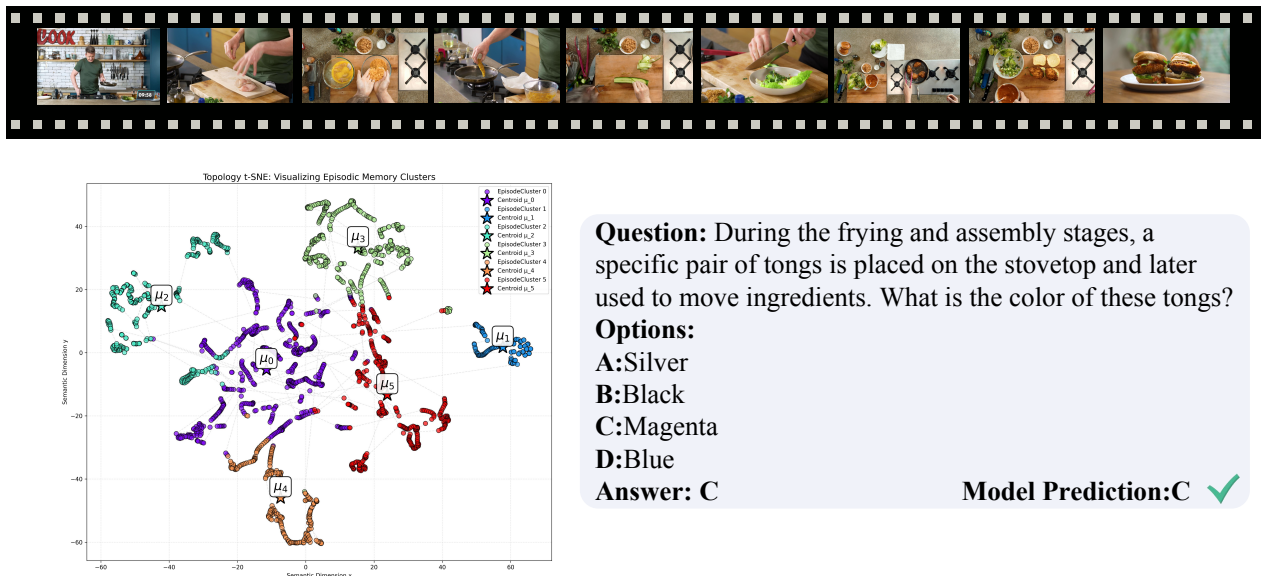


Figure 17. Interpretability analysis of the STM module.